

Superconducting Gap Modulation in Weak Stripe States

Masanori ICHIOKA* and Kazushige MACHIDA

Department of Physics, Okayama University, Okayama 700-8530

(Received March 15, 2002)

The superconducting gap modulation is investigated in the presence of a weak stripe structure, using the Bogoliubov-de Gennes theory on the two-dimensional Hubbard model with nearest-neighbor site pairing interaction. We calculate the local density of states and discuss the recently observed scanning tunneling spectroscopy spectra with four lattice periodicity on $\text{Bi}_2\text{Sr}_2\text{CaCu}_2\text{O}_{8+\delta}$. We also consider the spectral weight in the reciprocal space, where the Fermi surface and the superconducting gap are modulated by the band folding effect of the stripe structure.

KEYWORDS: stripe state, superconducting gap, Bogoliubov-de Gennes theory, local density of states, spectral weight

Recently, much attention has been focused on the stripe state of underdoped high- T_c cuprates. The stripe state was proposed to explain the static magnetic incommensurate structure observed in elastic neutron scattering experiments on $\text{La}_{2-x}\text{Sr}_x\text{CuO}_4$ (LSCO)¹⁻³⁾ and $\text{La}_{1.6-x}\text{Nd}_{0.4}\text{Sr}_x\text{CuO}_4$.^{4,5)} It is considered that doped holes are localized in the stripe region, which contributes to one-dimensional (1D) metallic conduction,⁶⁾ and the outside region of the stripe is an antiferromagnetic (AF) insulator. In $\text{YBa}_2\text{Cu}_3\text{O}_{7-\delta}$, inelastic neutron scattering experiments reported incommensurate fluctuations, which is consistent with the stripe concept.⁷⁻⁹⁾

Recently, the incommensurate charge modulation was also reported in $\text{Bi}_2\text{Sr}_2\text{CaCu}_2\text{O}_{8+\delta}$ (BSCCO). Scanning tunneling spectroscopy (STS) revealed modulated quasiparticle states with four unit-lattice periodicity surrounding a vortex core,¹⁰⁾ and recent STS experiments reported that the four unit-lattice periodic charge modulation survives even at zero field without a vortex.^{11,12)} In the Fourier component of the checker-board pattern, the peak intensity at either $\pi(\pm\frac{1}{4}, 0)$ or $\pi(0, \pm\frac{1}{4})$ is dominant (the lattice constant is taken as unity throughout this paper), meaning that we can assume a vertical stripe state and that the x - and the y -direction stripe layers are stacked layer by layer.

Our study is based on the self-consistent Hartree-Fock (HF) theory of the Hubbard model. It is believed that the stripe concept is valid beyond the HF approximation.¹³⁾ We can consider the metallic stripe state under the HF theory if we consider the realistic Fermi surface topology.^{14,15)} Once the density of states (DOS) remains at the Fermi energy (i.e., metallic state), we can produce superconductivity by introducing the pairing interaction, at least as a phenomenological model.¹⁶⁻¹⁹⁾ In the previous study on the superconducting state and the vortex state in the stripe state, we considered the case where the stripe order is stronger than the superconductivity.^{16,17)} However, experimental results on BSCCO suggest that the stripe order is not so great. Using the same method as ours, the stripe modulation around the vortex or the impurity center has been reproduced for

the weaker stripe case.²⁰⁾ Therefore, it is valuable to study the STS spectrum for the weak stripe state based on this theory.

In this work, we investigate how the superconducting gap is modulated by the stripe order with four (eight) unit-lattice charge (spin) periodicity at zero field. We use the Fermi surface topology and the electron filling ~ 0.88 appropriate to optimally doped BSCCO,²¹⁾ and study the weak stripe state in comparison with the superconductivity. We calculate the local density of states (LDOS), and discuss the STS spectrum on BSCCO. We also analyze the spectral weight, which is observed by angular-resolved photoemission spectroscopy (ARPES), to discuss how the Fermi surface and the superconducting gap in the reciprocal space are modulated by the weak stripe structure.

To consider the weak stripe modulation, we begin with the conventional Hubbard model on a two-dimensional square lattice, and introduce the mean field $n_{i,\sigma} = \langle a_{i,\sigma}^\dagger a_{i,\sigma} \rangle$ at the i -site, where σ is a spin index and $i = (i_x, i_y)$. We assume a singlet pairing interaction g_s between nearest-neighbor (NN) sites, because the coherence length is short in high- T_c cuprates. This type of pairing interaction produces d -wave superconductivity with the pairing function $\cos k_x - \cos k_y$. This gap function is confirmed by the ARPES experiment.²²⁾ The decomposition to the singlet and the triplet components of the pairing interaction is explained in ref. 23. Thus, the HF Hamiltonian is given by

$$\begin{aligned} \mathcal{H} = & - \sum_{i,j,\sigma} t_{i,j} a_{i,\sigma}^\dagger a_{j,\sigma} + U \sum_{i,\sigma} n_{i,-\sigma} a_{i,\sigma}^\dagger a_{i,\sigma} \\ & + g_s \sum_{i,j} (\Delta_{j,i}^\dagger a_{j,\downarrow} a_{i,\uparrow} + \Delta_{j,i} a_{j,\uparrow}^\dagger a_{i,\downarrow}^\dagger), \end{aligned} \quad (1)$$

with a creation (annihilation) operator $a_{i,\sigma}^\dagger$ ($a_{i,\sigma}$). For the transfer between nearest, second and third neighbor pairs (i,j) , $t_{i,j} = t, t'$ and t'' , respectively. Then, the dispersion is given by $\epsilon(\mathbf{k}) = -2t(\cos k_x + \cos k_y) - 4t' \cos k_x \cos k_y - 2t''(\cos 2k_x + \cos 2k_y)$. The singlet pairing potential is defined as $\Delta_{j,i} = g_s(\langle a_{j,\downarrow} a_{i,\uparrow} \rangle - \langle a_{j,\uparrow} a_{i,\downarrow} \rangle)$. When $n_{i,\sigma}$ and $\Delta_{\hat{e},j} (\equiv \Delta_{j,j+\hat{e}})$ have the N -

* E-mail address: oka@mp.okayama-u.ac.jp

site periodicity along the y -direction, we can write

$$n_{j,\sigma} = \sum_{0 \leq l < N} e^{il\mathbf{Q} \cdot \mathbf{r}_j} n_{\sigma,l\mathbf{Q}}, \quad (2)$$

$$\Delta_{\hat{e},j} = \sum_{0 \leq l < N} e^{il\mathbf{Q} \cdot \mathbf{r}_j} \Delta_{\hat{e},l\mathbf{Q}} \quad (\hat{e} = \hat{x}, \hat{y}), \quad (3)$$

with the ordering vector $\mathbf{Q} = 2\pi(\frac{1}{2}, \frac{1}{2} - \frac{1}{N})$. $\hat{x} = (1, 0)$ and $\hat{y} = (0, 1)$, respectively mean the next sites in the x - and y -directions. There is a relation $\Delta_{-\hat{e},j} = \Delta_{\hat{e},j-\hat{e}}$ in the singlet pairing.

After the Bogoliubov transformations $a_{j,\uparrow} = \sum_{\epsilon} (u_{\epsilon,j}\gamma_{\epsilon} - v'_{\epsilon,j}\gamma'_{\epsilon})$ and $a_{j,\downarrow} = \sum_{\epsilon} (v_{\epsilon,j}\gamma_{\epsilon} + u'_{\epsilon,j}\gamma'_{\epsilon})$, where ϵ is the label of the eigen states, we use the Fourier transformations from $u_{\epsilon,j}$ ($v_{\epsilon,j}$) to $u_{\epsilon,\mathbf{k}}$ ($v_{\epsilon,\mathbf{k}}$). We write $\mathbf{k} = \mathbf{k}_0 + m\mathbf{Q}$ ($m = 0, 1, \dots, N-1$), where \mathbf{k}_0 is within the reduced Brillouin zone of size $(2\pi)^2/N$. Then, the Bogoliubov-de Gennes (BdG) equation in reciprocal space is given by

$$\sum_{m'} \begin{pmatrix} K_{\uparrow,m,m'} & D_{m,m'} \\ D_{m,m'}^{\dagger} & -K_{\downarrow,m,m'}^* \end{pmatrix} \begin{pmatrix} u_{\alpha,\mathbf{k}_0,m'} \\ v_{\alpha,\mathbf{k}_0,m'} \end{pmatrix} = E_{\alpha,\mathbf{k}_0} \begin{pmatrix} u_{\alpha,\mathbf{k}_0,m} \\ v_{\alpha,\mathbf{k}_0,m} \end{pmatrix}, \quad (4)$$

where $K_{\sigma,m,m'} = [\epsilon(\mathbf{k}_0 + m\mathbf{Q}) - \mu]\delta_{m,m'} + U n_{-\sigma,(m-m')\mathbf{Q}}$ with chemical potential μ . $D_{m,m'} = g_s \sum_{\hat{e}=\hat{x},\hat{y}} (e^{i(\mathbf{k}_0+m'\mathbf{Q}) \cdot \hat{e}} + e^{-i(\mathbf{k}_0+m\mathbf{Q}) \cdot \hat{e}}) \Delta_{\hat{e},(m-m')\mathbf{Q}}$ with $u_{\epsilon,\mathbf{k}} = u_{\alpha,\mathbf{k}_0,m}$ and $v_{\epsilon,\mathbf{k}} = v_{\alpha,\mathbf{k}_0,m}$. The eigen-state ϵ is labeled by \mathbf{k}_0 and the eigen state α of eq. (4). Then, the wave function of the eigen states is given by

$$u_{\alpha,\mathbf{k}_0}(\mathbf{r}) = N_k^{-1/2} \sum_m u_{\alpha,\mathbf{k}_0,m} e^{i(\mathbf{k}_0+m\mathbf{Q}) \cdot \mathbf{r}}, \quad (5)$$

$$v_{\alpha,\mathbf{k}_0}(\mathbf{r}) = N_k^{-1/2} \sum_m v_{\alpha,\mathbf{k}_0,m} e^{i(\mathbf{k}_0+m\mathbf{Q}) \cdot \mathbf{r}}, \quad (6)$$

where $N_k = \sum_i 1 = \sum_{\mathbf{k}_0,m} 1$. We also obtain the same BdG equation as eq. (4) for $-v'^*_{\alpha,\mathbf{k}_0,m}$ and $u'^*_{\alpha,\mathbf{k}_0,m}$ but with the eigen-energy $-E'_{\alpha,\mathbf{k}_0}$. Then, $-v'^*_{\alpha,\mathbf{k}_0,m}$, $u'^*_{\alpha,\mathbf{k}_0,m}$, $-E'_{\alpha,\mathbf{k}_0}$ and γ' can, respectively, correspond to $u_{\alpha,\mathbf{k}_0,m}$, $v_{\alpha,\mathbf{k}_0,m}$, E_{α,\mathbf{k}_0} and γ . When there appears spin order, $u \neq u'$, $v \neq v'$, and $E \neq E'$, generally. The selfconsistent conditions are as follows,

$$\Delta_{\hat{e},l\mathbf{Q}} = \frac{1}{N_k} \sum_{\alpha,\mathbf{k}_0,m} [f(E_{\alpha,\mathbf{k}_0}) e^{i(\mathbf{k}_0+(m+l)\mathbf{Q}) \cdot \hat{e}} - f(-E_{\alpha,\mathbf{k}_0}) e^{-i(\mathbf{k}_0+m\mathbf{Q}) \cdot \hat{e}}] v_{\alpha,\mathbf{k}_0,m}^* u_{\alpha,\mathbf{k}_0,m+l}, \quad (7)$$

$$n_{\uparrow,l\mathbf{Q}} = \frac{1}{N_k} \sum_{\alpha,\mathbf{k}_0,m} u_{\alpha,\mathbf{k}_0,m}^* u_{\alpha,\mathbf{k}_0,m+l} f(E_{\alpha,\mathbf{k}_0}), \quad (8)$$

$$n_{\downarrow,l\mathbf{Q}} = \frac{1}{N_k} \sum_{\alpha,\mathbf{k}_0,m} v_{\alpha,\mathbf{k}_0,m}^* v_{\alpha,\mathbf{k}_0,m+l} f(-E_{\alpha,\mathbf{k}_0}), \quad (9)$$

with the Fermi distribution function $f(E)$.

The thermal Green's functions are given by $g_{11}(\mathbf{r}, \mathbf{r}', i\omega_n)$ $\sum_{\mathbf{k}_0,\alpha} u_{\alpha,\mathbf{k}_0}(\mathbf{r}) u_{\alpha,\mathbf{k}_0}^*(\mathbf{r}') / (i\omega_n - E_{\alpha,\mathbf{k}_0})$ and $g_{22}(\mathbf{r}, \mathbf{r}', i\omega_n) = \sum_{\mathbf{k}_0,\alpha} v_{\alpha,\mathbf{k}_0}(\mathbf{r}) v_{\alpha,\mathbf{k}_0}^*(\mathbf{r}') / (i\omega_n - E_{\alpha,\mathbf{k}_0})$ for up- and down-

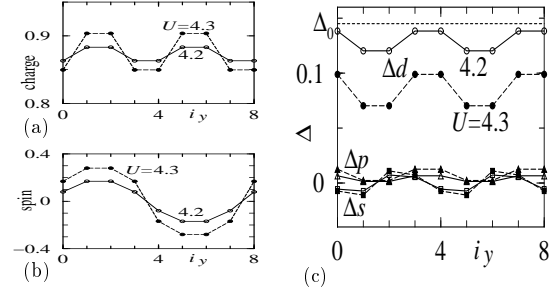


Fig. 1. (a) Profile of the charge density, n_i at the $(0, i_y)$ -site. $U = 4.2t$ (solid line) and $4.3t$ (dashed line). (b) Spin density $(-1)^{i_x+i_y} S_i$. (c) Superconducting pair potential for the d -wave $\Delta_{d,i}$ (circle), the s -wave $\Delta_{s,i}$ (square) and the p_y -wave $\Delta_{p,i}$ (tri-angle) components. Dotted line shows Δ_0 for the uniform state without stripe ($U = 0$).

spin electrons, respectively.²⁴⁾ Then, the LDOS $N(\mathbf{r}, E) = -\pi^{-1} \text{Im} g_{11}(\mathbf{r}, \mathbf{r}, i\omega_n \rightarrow E + i0^+) + \pi^{-1} \text{Im} g_{22}(\mathbf{r}, \mathbf{r}, -i\omega_n \rightarrow E + i0^+)$ is reduced to

$$N(\mathbf{r}, E) = \sum_l e^{il\mathbf{Q} \cdot \mathbf{r}} N(l\mathbf{Q}, E), \quad (10)$$

with the Fourier component

$$N(l\mathbf{Q}, E) = \frac{1}{N_k} \sum_{\mathbf{k}_0,\alpha,m} [u_{\alpha,\mathbf{k}_0,m}^* u_{\alpha,\mathbf{k}_0,m+l} \delta(E - E_{\alpha,\mathbf{k}_0}) + v_{\alpha,\mathbf{k}_0,m}^* v_{\alpha,\mathbf{k}_0,m+l} \delta(E + E_{\alpha,\mathbf{k}_0})]. \quad (11)$$

Similarly, from the Green's function $g(\mathbf{k}, i\omega_n) = N_k^{-1} \sum_{\mathbf{r}, \mathbf{r}'} e^{-i\mathbf{k} \cdot (\mathbf{r} - \mathbf{r}')} g(\mathbf{r}, \mathbf{r}', i\omega_n)$ in the \mathbf{k} -space, we obtain the spectral weight as¹⁵⁾

$$A(\mathbf{k}, E) = \sum_{\alpha,\mathbf{k}_0,m} [|u_{\alpha,\mathbf{k}_0,m}|^2 \delta(E - E_{\alpha,\mathbf{k}_0}) + |v_{\alpha,\mathbf{k}_0,m}|^2 \delta(E + E_{\alpha,\mathbf{k}_0})] \delta(\mathbf{k}_0 + m\mathbf{Q} - \mathbf{k}). \quad (12)$$

To reproduce the Fermi surface topology of BSCCO, we set $t' = -0.34t$, $t'' = 0.23t$ and $\mu \sim -0.9t$. The chemical potential μ is tuned in order to set the spatially averaged electron density $\bar{n}_i \sim 0.88$. The essential results of this study do not significantly depend on the choice of these parameter values. We consider the case of a vertical stripe state with the spin periodicity $N = 8$. The stripe states appear for $U > U_c \sim 4t$ on the BSCCO-type Fermi surface when $g_s = 0$. The critical U_c is larger than that of the LSCO-type Fermi surface.^{14,15)} We consider the superconducting state with $g_s = 0.8t$ and $T \sim 0$. In this case, the stripe state appears for $U > 4.1t$. We report the result for $U = 4.2t$ and $4.3t$. Since the stripe modulation is increased with raising U , the effect of the stripe is eminent for $U = 4.3t$.

Figures 1(a) and 1(b), respectively, show the profiles of the charge density $n_i = n_{i\uparrow} + n_{i\downarrow}$ and the spin density $S_i = \frac{1}{2}(n_{i\uparrow} - n_{i\downarrow})$. The domain wall of the AF is located at the bonds between $i_y=3$ and 4, and between $i_y=7$ and 8. Since the bond-centered stripe has lower energy than the site-centered stripe in our parameters, we report on the former case. Qualitatively, the same results are also obtained for the site-centered stripe case.

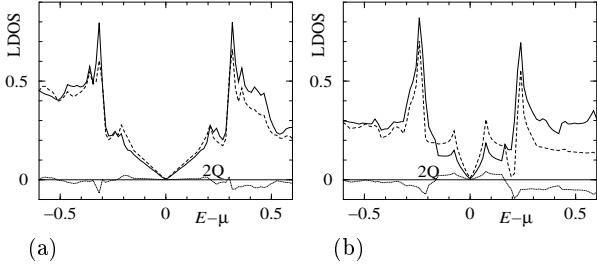


Fig. 2. Local density of states $N(\mathbf{r}_i, E)$ at the stripe site $i_y = 4$ (solid line) and the outside site $i_y = 5$ (dashed line). We also show the $2Q$ -Fourier component $N(2Q, E)e^{i5\pi/4}$ (dotted line). $U = 4.2t$ (a) and $4.3t$ (b).

At the stripe sites next to the domain wall, $1 - n_i$ is larger, i.e., doped holes are weakly accumulated. Corresponding to this stripe structure, the pair potential of the superconductivity is also modulated as shown in Fig. 1(c), where we show the components of d -wave $\Delta_{d,i} = (\Delta_{\hat{x},i} + \Delta_{-\hat{x},i} - \Delta_{\hat{y},i} - \Delta_{-\hat{y},i})/4$, extended s -wave $\Delta_{s,i} = (\Delta_{\hat{x},i} + \Delta_{-\hat{x},i} + \Delta_{\hat{y},i} + \Delta_{-\hat{y},i})/4$ and p_y -wave $\Delta_{p,i} = (\Delta_{\hat{y},i} - \Delta_{-\hat{y},i})/2$. The superconductivity is suppressed in total by the stripe formation. At the hole-rich stripe site, $\Delta_{d,i}$ has large amplitude. When $\Delta_{d,i}$ has a spatial variation, small $\Delta_{s,i}$ and $\Delta_{p,i}$ are also induced.

Figure 2 shows the LDOS at the stripe site and the outside site. In the presence of the stripe structure, there appear two peaks inside the gap of the d -wave superconductivity. These low energy peaks become larger at the outside site with weak $\Delta_{d,i}$. At the stripe site, the peak at the gap edge becomes sharp. We also present the Fourier component $N(2Q, E)e^{i5\pi/4} \propto N(i_y = 5, E) - N(i_y = 4, E)$, showing the difference of the LDOS between the stripe site and the outside site. The factor $e^{i5\pi/4}$ is multiplied so that the Fourier component becomes real. Recently, ref. 25 reported the calculation of the $2Q$ -component assuming charge density wave. Since the stripe site gains a large normal state DOS with hole accumulation, the DOS above the superconducting gap is larger at the stripe site in Fig. 2. When the calculated spectrum is compared with the STS spectrum,^{11,12} they both show that the $2Q$ -Fourier component is positive (negative) at lower (higher) energies. However, the weights of the positive and negative parts of the $2Q$ -component are quantitatively different. In the STS spectrum, the weight of the negative $2Q$ -component at higher energies is small, because the peak of the gap edge is broad at the site with a large superconducting gap. In our calculation, the peak at the gap edge becomes sharp, and the weight of the negative $2Q$ -component is large. We give some discussion as follows with respect to this inconsistency.

(i) In order to reproduce the observed STS spectrum, we need to consider additional effects of broadening the sharp gap edge at the site with a larger superconducting gap, for example, broadening by impurity scattering, whose contribution may be larger at the site with a large normal state DOS.

(ii) The peak inside the gap (the peak at gap-edge) at the outside (stripe) site also appears at the stripe (outside) site, meaning that the peak state extends to the

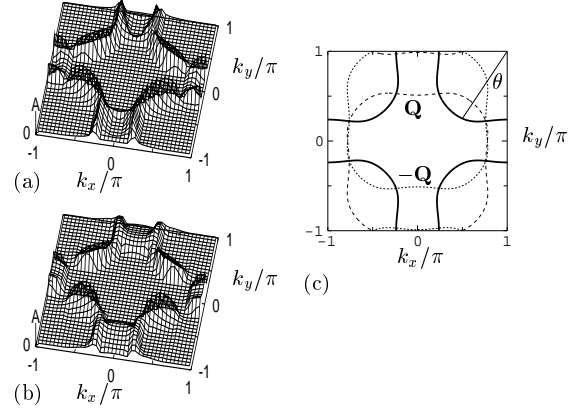


Fig. 3. Spectral weight at Fermi energy in the regions $|k_x| \leq \pi$ and $|k_y| \leq \pi$. We plot integrated $A(\mathbf{k}, E)$ within the energy range $|E - \mu| < 0.5t$. $U = 4.2t$ (a) and $4.3t$ (b). (c) Original Fermi surface (bold line) and $\pm Q$ -shifted ones (dotted and dashed lines).

adjacent outside (stripe) site. However, we see only one peak (higher or lower energy) at each site in the STS spectrum. This suggests that the coherence of the peak state is restricted to within a few sites by the smearing effect of (i), or by other effect which confines the peak state to within a few sites.

(iii) We assume that the pairing interaction is constant. Then, the site dependence of $\Delta_{d,i}$ comes from the site dependence of the DOS. We can consider the possibility that the pairing interaction depends on the local hole density, having an additional effect on the gap inhomogeneity. This may be related to the inter-site coherence of the peak state as noted in (ii).

(iv) In our calculation, we assume the incommensurate spin order in addition to the charge order. The STS observes the charge order with the ordering vector $2Q$. However, the spin order with the ordering vector Q has not been confirmed experimentally. We expect that the ordering with Q can be detected by ARPES, as discussed later.

Next, we discuss how the gap modulation due to the stripe structure appears in the reciprocal space. The wave number \mathbf{k} -resolved DOS is the spectral weight $A(\mathbf{k}, E)$, which is obtained with the same wave function used in the LDOS calculation. When the system has a periodic structure, the band folding effect appears in $A(\mathbf{k}, E)$. Figures 3(a) and 3(b) show the spectral weight at the Fermi energy μ in the stripe state, integrating $A(\mathbf{k}, E)$ in the energy width $\pm 0.5t$ around μ . In addition to the DOS at the original Fermi surface, there appears small DOS near $(\pi, 0)$ and $(0, \pi)$ in the stripe state. As schematically presented in Fig. 3(c), this is due to $\pm Q$ -shifted Fermi surfaces. To induce new DOS by band folding, finite DOS is necessary near the Fermi energy in the original dispersion $\epsilon(\mathbf{k})$. Around $(\pi, 0)$ and $(0, \pi)$, there is large DOS at $E \sim \mu - 1.0t$ due to the van Hove singularity in our dispersion. It is worth noting that the

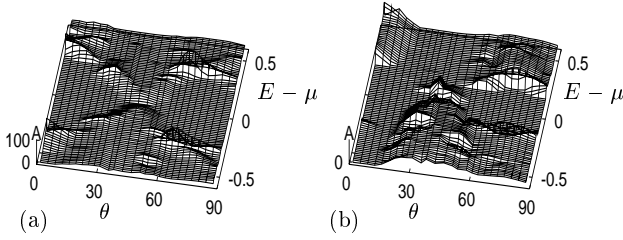


Fig. 4. The superconducting gap along the Fermi surface. We plot $A(\mathbf{k}, E)$ at \mathbf{k} along the Fermi surface. Wave number \mathbf{k} is specified by the angle θ from (π, π) , as shown in Fig. 3(c). $U = 4.2t$ (a) and $4.3t$ (b).

Fermi surface near $(\pi, 0)$ and $(0, \pi)$ is still the subject of discussion, because additional spectral weight appears there.^{26–28} The spectral weight for the (π, π) -shifted Fermi surface could appear due to AF fluctuations as observed in the ARPES experiment.²⁸ If the AF fluctuation is changed to an incommensurate one with ordering vector \mathbf{Q} , we expect to observe the spectral weight for a \mathbf{Q} -shifted Fermi surface instead of a (π, π) -shifted one.

To discuss the superconducting gap structure in the reciprocal space, we show $A(\mathbf{k}, E)$ along the Fermi surface in Fig. 4. The DOS vanishes when $|E - \mu|$ is smaller than the superconducting gap, and has a peak at the gap edge. In the uniform state without the stripe, the gap is given by $|\cos k_x - \cos k_y|$, which has a node at $\theta = 45^\circ$. In the presence of the stripe, the gap is modulated as shown in Fig. 4. Around $\theta = 15^\circ$, the Fermi surface DOS vanishes upon the reconnection between the original dispersion and the $\pm\mathbf{Q}$ -shifted dispersions. For $\theta > 60^\circ$, θ -dependence of the gap becomes flat. When the x - and the y -direction stripe layers are stacked layer by layer in the sample, or when there is a domain structure for the x - and the y -direction stripe regions within a layer, we observe an overlap of the spectral weights for both direction stripe states, i.e., $[A(\mathbf{k}, E) + A(k_x \leftrightarrow k_y, E)]/2$.

When the stripe modulation becomes strong with increasing U in our system, the DOS at the Fermi energy is reconstructed and they form a 1D Fermi surface at $k_x = \pm\pi/4$, but the DOS vanishes near $(\pi/2, \pi/2)$, as suggested in refs. 15 and 29. In this case, the superconducting gap in the LDOS $N(\mathbf{r}_i, E)$ has a small full gap, because the low-energy state near the gap node around $(\pi/2, \pi/2)$ vanishes in reciprocal space. This spectrum is seen in Fig. 3 of ref. 17. There, the spectrum at the site far from the vortex is almost the same as that of the zero-field case without a vortex.

In summary, we investigate the superconducting gap modulation in the presence of a weak stripe structure, using the BdG theory. From the same wave functions, the LDOS related to the STS spectrum and the spectral weight related to ARPES are calculated. In the former, there appear new peaks inside the superconducting

gap. In the latter, there appears the effect of band folding caused by the stripe structure. On the basis of our results, we have discussed the STS spectrum with four

unit-lattice periodicity on BSCCO.^{11,12)}

We would like to thank E. Kaneshita, M. Takigawa and N. Nakai for valuable discussions.

- 1) M. Matsuda, M. Fujita, K. Yamada, R. J. Birgeneau, M. A. Kastner, H. Hiraka, Y. Endoh, S. Wakimoto and G. Shirane: Phys. Rev. B **62** (2000) 9148.
- 2) S. Wakimoto, G. Shirane, Y. Endoh, K. Hirota, S. Ueki, K. Yamada, R. J. Birgeneau, M. A. Kastner, Y. S. Lee, P. M. Gehring and S. H. Lee: Phys. Rev. B **60** (1999) 769.
- 3) T. Suzuki, T. Goto, K. Chiba, T. Shinoda, T. Fukase, H. Kimura, K. Yamada, M. Ohashi and Y. Yamaguchi: Phys. Rev. B **57** (1998) R3229.
- 4) J. M. Tranquada, B. J. Sternlieb, J. D. Axe, Y. Nakamura and S. Uchida: Nature **375** (1995) 561.
- 5) J. M. Tranquada, J. D. Axe, N. Ichikawa, A. R. Moodenbaugh, Y. Nakamura and S. Uchida: Phys. Rev. Lett. **78** (1997) 338.
- 6) T. Noda, H. Eisaki and S. Uchida: Science **286** (1999) 265.
- 7) H. A. Mook, P. Dai, S. M. Hayden, G. Aeppli, T. G. Perring and F. Doğan: Nature **395** (1998) 580.
- 8) H. A. Mook, P. Dai, F. Doğan and R. D. Hunt: Nature **404** (2000) 729.
- 9) M. Arai, T. Nishijima, Y. Endoh, T. Egami, S. Tajima, K. Tomimoto, Y. Shinohara, M. Takahashi, A. Garrett and S. M. Bennington: Phys. Rev. Lett. **83** (1999) 608.
- 10) J.E. Hoffman, E.W. Hudson, K.M. Lang, V. Madhavan, H. Eisaki, S. Uchida and J.C. Davis: Science **295** (2001) 466.
- 11) C. Howald, H. Eisaki, N. Kaneko and A. Kapitulnik, cond-mat/0201546.
- 12) K.M. Lang, V. Madhavan, J.E. Hoffman, E.W. Hudson, H. Eisaki, S. Uchida and J.C. Davis: Nature **415** (2002) 412.
- 13) J. Zaanen and A. M. Oleś: Ann. Phys. **5** (1996) 224.
- 14) K. Machida and M. Ichioka: J. Phys. Soc. Jpn. **68** (1999) 2168.
- 15) M. Ichioka and K. Machida: J. Phys. Soc. Jpn. **68** (1999) 4020.
- 16) M. Ichioka and K. Machida: Physica B **281&282** (2000) 804.
- 17) M. Ichioka, M. Takigawa and K. Machida: J. Phys. Soc. Jpn. **70** (2001) 33.
- 18) I. Martin, G. Ortiz, A. V. Balatsky and A. R. Bishop: Europhys. Lett. **56** (2001) 849.
- 19) A. Himeda, T. Kato and M. Ogata: Phys. Rev. Lett. **88** (2002) 117001.
- 20) J.-X. Zhu, I. Martin and A.R. Bishop: cond-mat/0201519.
- 21) A.A. Kordyuk, S.V. Borisenko, M.S. Golden, S. Legner, K.A. Nenkov, M. Knupfer, J. Fink, H. Berger, L. Forró and R. Follath: cond-mat/0201485.
- 22) H. Ding, M.R. Norman, J.C. Campuzano, M. Randeria, A.F. Bellman, T. Yokoya, T. Takahashi, T. Mochiku and K. Kadowaki: Phys. Rev. B **54** (1996) 9678.
- 23) M. Takigawa, M. Ichioka and K. Machida: Phys. Rev. B **65** (2002) 014508.
- 24) M. Takigawa, M. Ichioka and K. Machida: J. Phys. Soc. Jpn. **69** (2000) 3943.
- 25) A. Polkovnikov, M. Vojta and S. Sachdev: cond-mat/0203176.
- 26) Y.-D. Chuang, A.D. Gromko, D.S. Dessau, Y. Aiura, Y. Yamaguchi, K. Oka, A.J. Arko, J. Joyce, H. Eisaki, S. Uchida, K. Nakamura and Y. Ando: Phys. Rev. Lett. **83** (1999) 3717.
- 27) H.M. Fretwell, A. Kaminski, J. Mesot, J.C. Campuzano, M.R. Norman, M. Randeria, T. Saito, R. Gatt, T. Takahashi and K. Kadowaki: Phys. Rev. Lett. **84** (2000) 4449.
- 28) S.V. Borisenko, M.S. Golden, S. Legner, T. Pichler, C. Dür, M. Knupfer, J. Fink, G. Yang, S. Abell and H. Berger: Phys. Rev. Lett. **84** (2000) 4453.
- 29) X.J. Zhou, P. Bogdanov, S.A. Kellar, T. Noda, H. Eisaki, S. Uchida, Z. Hussain and Z.-X. Shen: Science **286** (1999) 268.